Adsorption of Rose Bengal on a self-assembled fibrillar network affords a thermally switchable oxygenation photocatalyst and a thermochromic soft material

*Carla Arnau-del-Valle, Carles Felip-León, César A. Angulo-Pachón, Francisco Galindo and Juan F. Miravet**

Department of Inorganic and Organic Chemistry, Universitat Jaume I , Avda. Sos Baynat s/n, 12071 Castelló de la Plana, Spain

E-mail: Francisco.galindo@uji.es, miravet@uji.es

Keywords: supramolecular gels, photosensitizers, self-assembly, thermochromism, soft materials

Rose Bengal (RB) can be homogeneously dispersed in dichloromethane by its adsorption on the fibrillar network of a molecular gel formed in this solvent. The RB loaded gel was visualized by confocal scanning laser microscopy, revealing homogenous distribution all over the self-assembled fibers. Thermal gel disassembly provokes discoloration of the system because of protonation of RB by the acidic molecular gelator. Thermochromism was evaluated by UV-Vis spectroscopy, showing that color change is fully reversible and associated with gel assembly/disassembly, as corroborated by ^{1}H NMR determination of the amount of free gelator. Singlet oxygen photogeneration from the RB-loaded gel was assayed using 9,10-dimethylanthracene as a $^{1}O_2$ trap. It was found that the photosensitizing activity of the system is on /off thermally switched, controlled by reversibly gel formation, resulting in a smart thermoresponsive photocatalytic material.

1. Introduction

The emergence of catalytic properties associated with self-assembly represents an exciting topic.[1, 2] For example, the possible role in the origin of life of catalytic self-assemblies formed by amyloids,[3] lipids[4] or small peptides[5] has been discussed. The catalytic activity of self-assembled short peptides in different reactions has been reviewed recently, showing in some cases efficiency comparable to that found in enzymes.[6] Self-assembly of a variety of molecules into chiral nanostructures such as nanotubes or vesicles, among others, has been shown to produce remarkable enantioselective catalysts.[7]

A fascinating case of self-assembly is that resulting in molecular gels. They are formed through aggregation of low molecular mass species that form sample spanning fibrillar networks. These soft materials have been extensively studied during the last two decades.[8-11] Molecular gels are intrinsically stimuli-responsive, and gel to solution transition can be triggered by different stimuli such as light, pH, salts or heat, among others.[12-14] Molecular gel formation has been reported in a few cases to produce emergence or improvement of catalytic activity. A molecular gel formed by an L-proline derivative resulted in catalytic fibers for the nitroaldol reaction.[15] A peptide amphiphile containing histidine[16] and an imidazole appended molecular gelator accelerated ester hydrolysis when aggregated in nanofibers.[17] Aldol reaction was catalysed by different molecular gels containing L-proline moieties [18-20] and orthogonal fibrillization afforded cooperative acid and basic catalysis.[21, 22] Molecular gels have also been used as media for several photochemical and photophysical studies, leading either to fundamental knowledge or to practical applications.[23, 24]

Singlet oxygen, $^1O_2$, constitutes is a highly reactive oxygen species that has received enormous interest associated with its participation in many biological processes. In vivo generation of $^1O_2$ include enzymatic pathways which have been emulated, for example, for the development of transient supramolecular hydrogels,[25] and photoactivated reactions. A variety of artificial photosensitizers of $^1O_2$ have been developed, mimicking photobiological

processes.[26] Photosensitized generation of $^1O_2$ is the base of anticancer[27, 28] and antimicrobial[29] photodynamic therapy. In particular, Rose Bengal (RB) see Scheme 1) is a dianionic photosensitizer with strong absorption at ca. 550 nm whose first excited state ($^1RB^{2-*}$) experiments intersystem crossing (ISC) to the excited triplet state ($^3RB^{2-*}$), which can be quenched very efficiently by oxygen, producing singlet oxygen ($^1O_2$).[30] As a result of these properties, RB has been widely used in photodynamic therapy[31] and organic synthesis.[32] From the practical point of view, to circumvent the limitations of photochemistry in solution, RB has been immobilized, principally in polystyrene-based polymeric supports, leading to heterogeneous photosensitizers.[33-35]

Thermochromism was defined by J.H. Day in a seminal work as the reversible dependence of color on temperature.[36] The incorporation of thermochromic dyes or liquid crystals into polymers has received much attention.[37] In particular, thermochromism in polymeric hydrogels was firstly described by Seeboth *et al.* They studied the thermochromic behavior of a betaine dye and cresol red, based on proton-transfer phenol-phenolate equilibrium, embedded in a polyvinyl alcohol/borax/surfactant hydrogel matrix. They found that polymer networks were a decisive part of the thermochromic system by establishing co-operative linkages by hydrogen bonding.[38] To date, similar strategies were carried out for designing thermochromic polymers, and different materials have been developed based on this finding, such films that present thermal erasable imaging[39] or thermo-controlled transparency.[40] However, thermochromic behavior in molecular materials has been scarcely studied so far. Chromogenic compounds bromophenol blue and polyoxomolybdate complexes were described to experiment color change associated with the formation of, respectively, molecular hydrogels[41] and organogels.[42]

Here we report on how molecular gel formation by compound 1 (Scheme 1) in dichloromethane activates RB reversibly as a photosensitizer. The thermal regulation of $^1O_2$ photogeneration has only been reported for a copolymer of RB and N-isopropylacrylamide[43], but there is no precedent, up to our knowledge, of thermal control of photosensitizing activity

by a molecular gel assembly/disassembly process. Additionally, the hybrid soft material described here behaves as a thermochromic material.

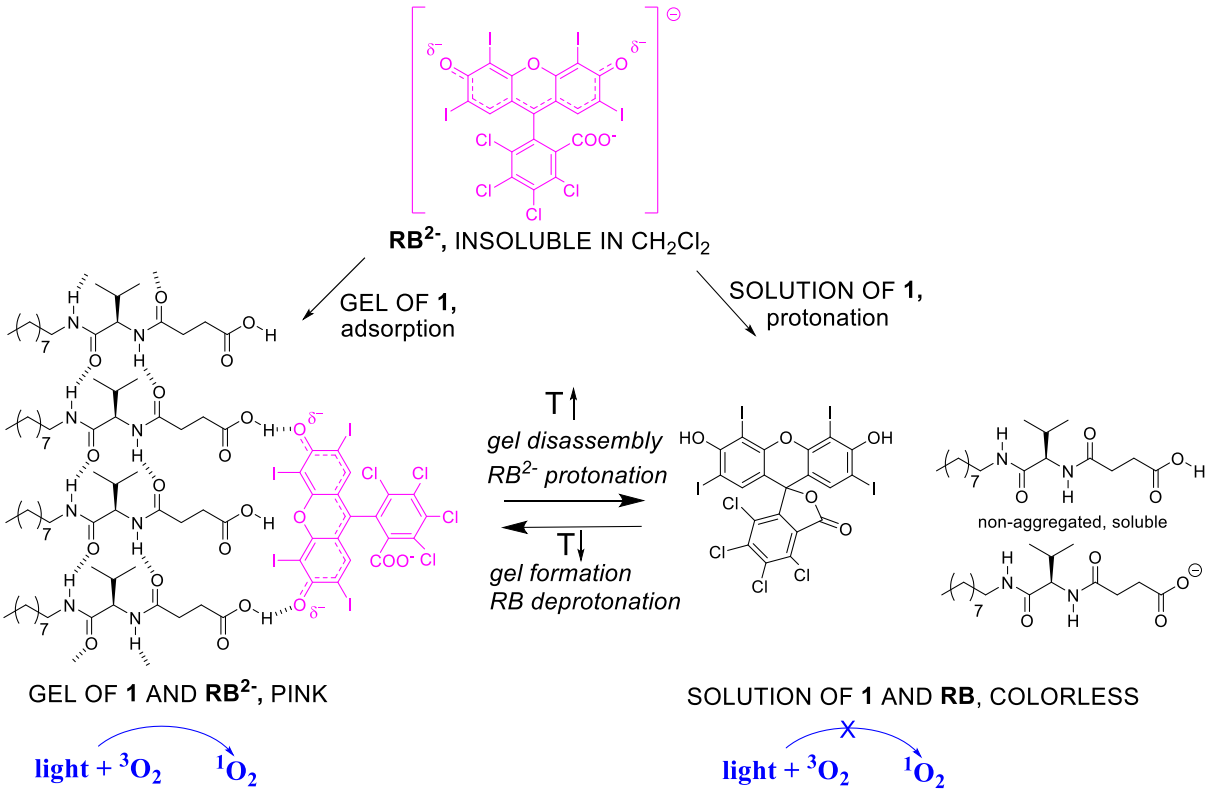

Scheme 1. Depiction of the equilibrium proposed for the system **1** + RB.

2. Results and discussion

Compound **1** is constituted by an L-valine unit modified as a nonylamide at the carboxylic acid unit and acylated with succinic acid at the amine function. The formation of nanogel particles and macroscopic gels by **1** has been recently reported by us.[44] In previous work, related amphiphilic structures with a variation of the aliphatic chain length or the amino acid have been shown to form organo and hydrogels.[45, 46] An aggregation model based in multiple H-bonds has been proposed for this family of compounds as depicted in Scheme 1.

Gel formation in dichloromethane was assayed by cooling to room temperature solutions of **1**, yielding optically transparent gels with a minimum gelation concentration of 10 mM. This solvent was chosen for the detailed study that follows because of the moderate temperature at

which gel disassembly takes place. A related behavior was observed in toluene, but gel disassembly in this solvent takes place above 90ºC.

Although the sodium salt of the dianionic form of Rose Bengal (RB^{2-}) is insoluble in dichloromethane, upon heating to 40ºC in a closed vial in the presence of **1** (14.4 mM) a transparent, almost colorless, solution was obtained ([RB] = 7.7 μM). The soluble, colorless, form of RB should be ascribed, in analogy to fluorescin, to the neutral lactone RB depicted in Scheme 1, which only is formed from the neutral, diprotonated fluorescein species.[47] As outlined in Scheme 1, most likely a proton transfer from the carboxylic acid groups of the gelator to RB^{2-} is taking place, producing the dichloromethane soluble species RB. A similar solubilization process took place in the presence of acetic acid, yielding an almost colorless stable solution at room temperature and supporting that protonation of RB^{2-} is taking place. It could also be considered that the formation of mixed aggregates between RB and the amphiphilic gelator **1** may occur, contributing to the stabilization of the neutral lactonic form of RB. Remarkably, when the solution of RB^{2-} in the presence of **1** is cooled down to room temperature, a homogeneous optically transparent pink gel is obtained (see inset in Figure 2). T_{gel} for the system **1**+RB was determined by UV-Vis turbidimetry to be 33.8 ± 1.4 ºC (baseline monitored at 800 nm, see SI) a value slightly higher than that found for **1** in the absence of RB, 30.8 ± 0.5 ºC.

As depicted in Scheme 1, this behavior can be rationalized considering that aggregation of **1** reduces its acidity in dichloromethane, resulting in the deprotonation and ring-opening of colorless RB back to the pink form RB^{2-}, initially insoluble in this solvent. The homogeneous and optically clear characteristics of the gel indicate that adsorption of RB^{2-} on the self-assembled fibers precludes its aggregation into insoluble particles. The adsorption would, most likely, be driven by hydrogen bonding of the negatively charged phenolic units of RB with the hydrogen atoms of the carboxylic acid units of the gelator.

The homogenous distribution of RB^{2-} on the fibrillar network of the gel was nicely visualized by confocal laser scanning microscopy, taking advantage of the fluorescence of RB^{2-} (Figure 1)

The gel formed by RB and **1** constitutes a soft thermochromic material. Variable temperature studies of the change from pink to almost colorless systems were carried out measuring the absorption at 560 nm (Figure 2). A sigmoidal dependence of the absorption with temperature was observed. Importantly, the thermochromic behavior is reversible, and five heating-cooling cycles were run without any significant fatigue of the system (Figure 2).

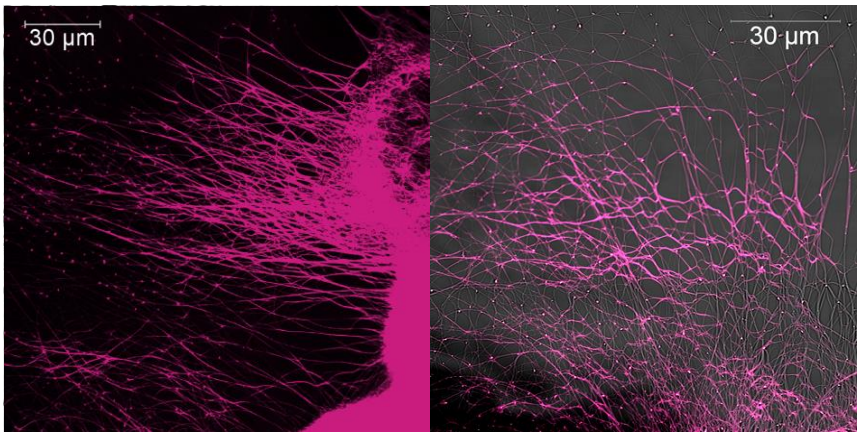

Figure 1. Confocal laser scanning microscopy images of gel of **RB@1** (λ_{ex} = 561 nm, λ_{em} = 529 nm-649 nm) [RB] = 62 µM , [**1**] = 14.4 mM in CH_2Cl_2.

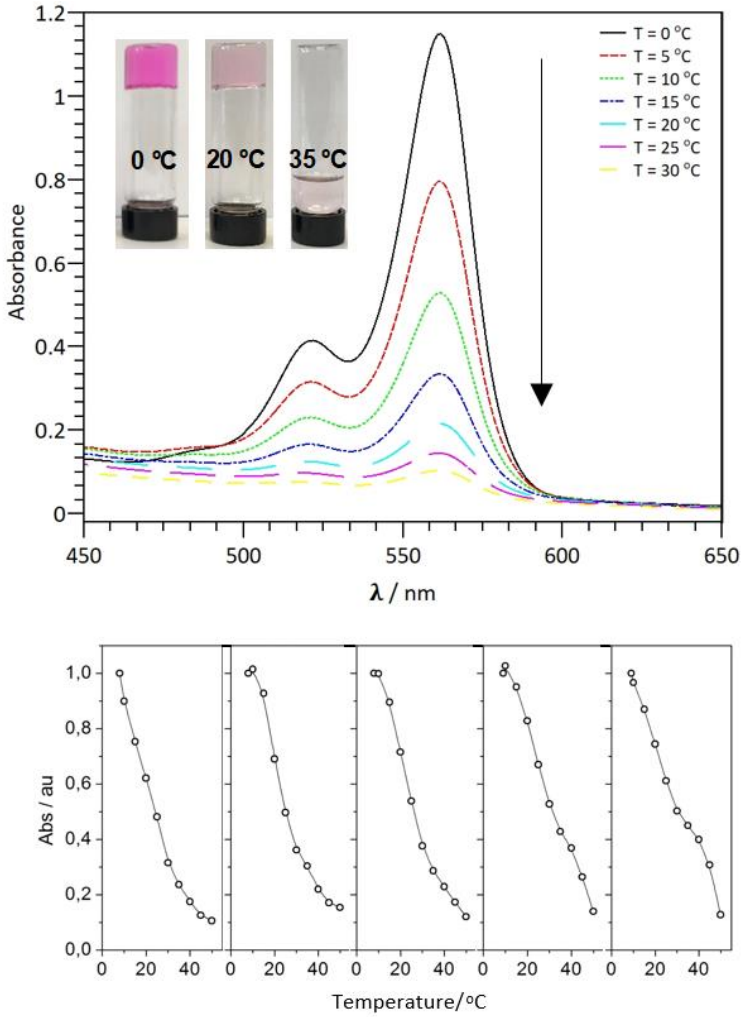

Figure 2. Top: UV-Vis spectra of gels of RB@**1** in CH_2Cl_2 at different temperatures showing photochromic behavior upon gel assembly/disassembly. Bottom: heating-cooling cycles of photochromic gels followed by UV-Vis absorption at λ_{abs} = 560 nm. [RB] = 7.7 µM, [**1**] = 14.4 mM in CH_2Cl_2. ΔT = 5 ºC.

The progressive discoloration observed should be linked to the disassembly of the gel fibers being the system a solution above ca. 30 ºC. Indeed, the variation of solubility of 1 with the temperature determined by ^{1}H NMR, correlates well with the changes observed by UV-Vis spectroscopy (Figure 3).

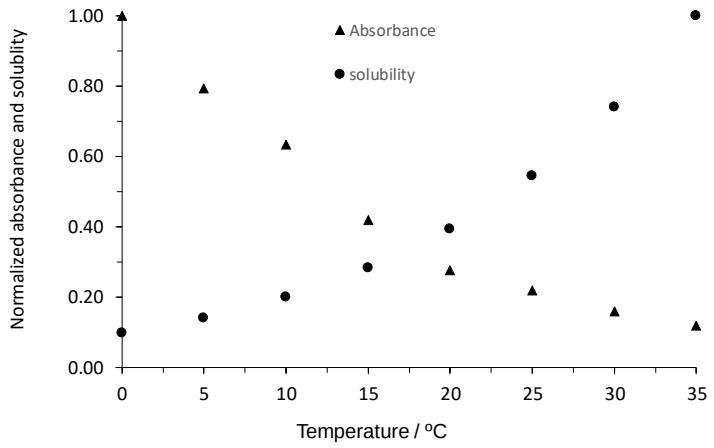

Figure 3. Comparison of UV-absorbance at 560 nm and solubility determined by ^{1}H NMR for the system RB-**1**. [RB] = 7.7 µM, [**1**] = 14.4 mM in CH_2Cl_2

Photogeneration of singlet oxygen ($^1O_2$) by the system **1**+RB upon irradiation with visible light was assessed using a benchmark photooxidation reaction that uses 9,10-dimethylanthracene (DMA) as a singlet oxygen trap. The UV-Vis absorption of DMA above 300 nm disappears upon the formation of an endoperoxide with $^1O_2$.[48] The rate of this reaction can be fitted to a pseudo-first-order model (see SI for details). Photooxidation kinetics was measured in the temperature range of 0-35 ºC (Figure 4). As expected, the rate of singlet oxygen generation follows the same trend observed for the color change (see SI). The kinetic constant at 0 ºC (0.098 min^{-1}, $t_{1/2}$ = 7 min) is almost an order of magnitude higher than that of the solution at 35 ºC (0.0116 min^{-1}, $t_{1/2}$ = 60 min). The variation of $^1O_2$ production rate with temperature correlates well with that observed for the UV-Vis absorbance of Rose Bengal (see the comparison at SI). Below 5 ºC the photooxidation constant reaches a plateau which would correspond to the adsorption of RB on the gel fibers which is poorly active as a photosensitizer. This effect could be the result of dimer formation by adsorbed RB, resulting in quenched photosensitizing activity.[49]

On the other hand, in a control experiment, using RB^{2-} solubilized in dichloromethane with the help of tetrabutylammonium cation, the rate of photoxygenation was poorly temperature dependent, with values at 5ºC and 35 ºC of 0.073 min^{-1} and 0.082 min^{-1} respectively. The

invariance of singlet oxygen production by these soluble species at different temperatures indicates that the amount of dissolved oxygen in the medium is hardly affected by the temperature increase.

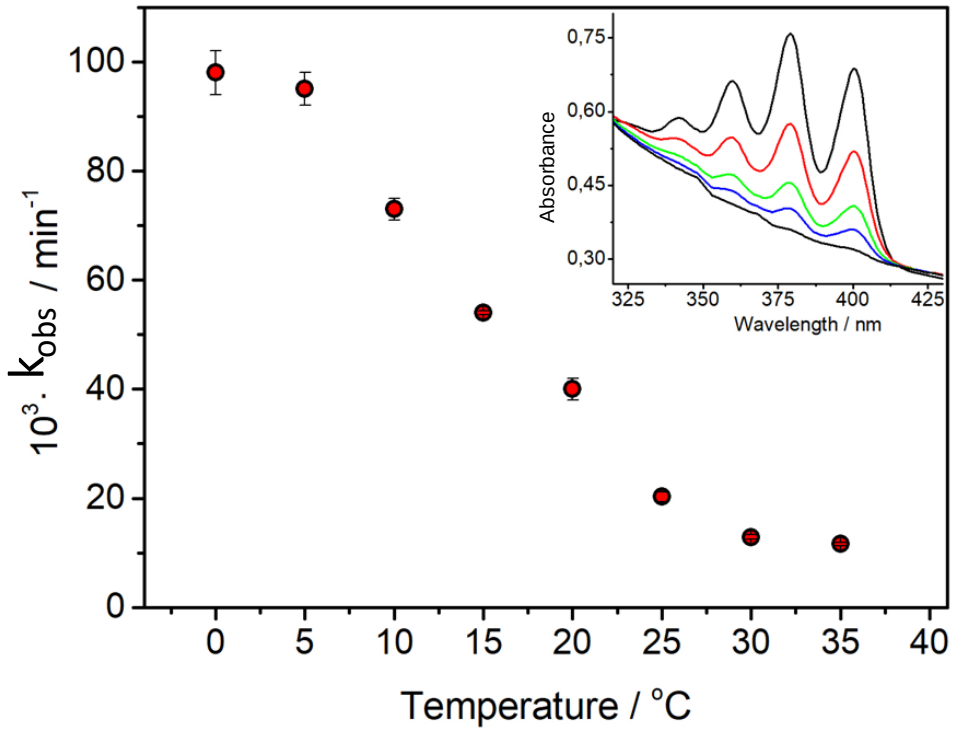

Figure 4. Temperature-dependent kinetics of DMA photooxidation performed by gels of **1**@RB in CH_2Cl_2; Inset: UV-Vis spectra at 10 ºC.

3. Conclusions

Summarizing, the results obtained indicate that gelator **1** is capable of solubilizing RB^{2-} in dichloromethane above ca. 30ºC. This behavior is the result of the acidic properties of **1** in solution, promoting the formation of the colorless lactone form of RB. At room temperature, **1** forms self-assembled fibers that present enhanced basicity and preclude the protonation of RB^{2-}. The fibrillar network adsorbs RB^{-2}, resulting in homogeneously pink-colored, transparent gels which can be thermally transformed, reversibly, into almost colorless solutions, constituting a soft thermochromic material.

The gel **1**-RB is found to be an efficient $^1O_2$ photosensitizer whose activity is heavily regulated by temperature, being the $^1O_2$ production almost completely halted at 35 ºC.

The presented system constitutes a first example and a proof of concept of how molecular gel assembly/disassembly can be used to modulate the catalytic activity of species present in the medium, producing smart, thermoresponsive, soft photocatalytic materials.

4. Experimental Section

Commercial reagents 9,10-dimethylanthracene (DMA), Rose Bengal disodium salt (RB) and all the solvents have been used as received. Solvents for optical measurements were spectroscopic grade. NMR spectra were recorded at 400 MHz (^{1}H NMR) in a Bruker Avance III HD 400 MHz apparatus. Solutions and suspensions were measured in a JASCO V-630 apparatus for UV-Vis measurements, using 3 mL quartz cuvettes with 10 mm path length.

Confocal laser scanning microscopy (CLSM) was performed on an inverted confocal microscope Leica TCS SP8. Images were obtained with an HCX PL APO CS 63x/0.40 OIL. Excitation was carried out with an argon laser (561 nm) and data acquisition with a PMT detector (λ_{em} = 529 nm-649 nm). The gels were observed directly on sterilized Ibidi m-Slide 8 Well Glass Bottom: # 1.5H (170 mm 5 mm) Schott glass.

Compound **1** was synthetized as previously described.[44]

For the determination of minimum gelation concentration of **1**, different amounts of **1** were weighted inside of cylindrical glass vial (diameter = 1.5 cm). Then 1 mL of solvent was added, and the vial closed hermetically. This mixture was dissolved by heating up to 40ºC, and afterward, the mixture was left at room temperature for 10 minutes. The formation of a gel was checked by turning the vial upside down.

The thermal stability of the gels was tested using UV-vis absorption measurements at 800 nm. The transmitted light is scattered in the gel, but not when it is a solution.

For the preparation of RB loaded gels, a stock solution was prepared by weighing 6.00 mg of RB in 50 mL of ethanol (EtOH). An aliquot of such stock solution (125 µL) was added into a glass vial, and the solvent was evaporated under airflow. Then, 10.00 mg of **1** and 2 mL of dichloromethane were added into the glass vial. The mixture was dissolved by heating, and then

it was left at room temperature for 10 min. The formation of the gel was checked by turning the vial upside down.

RB^{2-} could be solubilized in dichloromethane for the control experiments by addition of 1 µL of tetrabutylammonium hydroxide. For control experiments involving protonated RB, 1.6 µL of glacial acetic acid were added either to a suspension of RB in DCM or to the gel of **1**+RB.

Photo-oxygenation reactions were performed inside closed 3 mL fluorescence quartz cuvettes containing the gel and the singlet oxygen trap 9,10-dimethylanthracene (DMA) (0.05 mM, aerated solution). Irradiations were carried out using two LED lamps (11 W each, Lexman, ca. 400–700 nm emission output; 15.6 mW/cm^2) placed 1 cm away from the quartz cell. The evolution of the photoreactions was monitored over time using UV-vis absorption spectrophotometry (decrease of absorbance at 376 nm). The initial points of the kinetic traces were fitted to a pseudo-first order model ($\ln C/C_0 = - k_{obs} \cdot t$, where C is the concentration of DMA at a specific time t, and C_0 is the initial concentration of DMA).

For the determination of the variation of solubility of **1** with temperature, the gel was prepared inside of the NMR tube ([**1**] = 15 mM) using as solvent CD_2Cl_2 with tetrachloroethane as an internal standard for integration. Proton spectra were collected at different temperatures letting the sample stabilize at the corresponding temperature for 10 minutes.

5. Acknowledgments

The authors acknowledge financial support from Ministerio de Economía y Competitividad of Spain (grant CTQ2015-71004-R) and Universitat Jaume I (grants UJI-B2018-54; UJI-B2018-30).

6. Data availability

The raw/processed data required to reproduce these findings cannot be shared at this time due to time limitations**.**

7. References

1. M. Raynal, P. Ballester, A. Vidal-Ferran and P. W. N. M. Van Leeuwen, *Chem. Soc. Rev.*, 2014, **43**, 1734-1787.
2. Y. Tu, F. Peng, A. Adawy, Y. Men, L. K. E. A. Abdelmohsen and D. A. Wilson, *Chem. Rev.*, 2016, **116**, 2023-2078.
3. T. O. Omosun, M. C. Hsieh, W. S. Childers, D. Das, A. K. Mehta, N. R. Anthony, T. Pan, M. A. Grover, K. M. Berland and D. G. Lynn, *Nat. Chem.*, 2017, **9**, 805-809.
4. D. Lancet, R. Zidovetzki and O. Markovitch, *J. Royal Soc. Interface*, 2018, **15**, 159.
5. O. Carny and E. Gazit, *The FASEB Journal*, 2005, **19**, 1051-1055.
6. O. Zozulia, M. A. Dolan and I. V. Korendovych, *Chem. Soc. Rev.*, 2018, **47**, 3621-3639.
7. J. Jiang, G. Ouyang, L. Zhang and M. Liu, *Chem. Eur. J.*, 2017, **23**, 9439-9450.
8. A. R. Hirst, B. Escuder, J. F. Miravet and D. K. Smith, *Angew. Chem. Int. Ed.*, 2008, **47**, 8002-8018.
9. J. W. Steed, *Chem. Commun.*, 2011, **47**, 1379-1383.
10. X. Du, J. Zhou, J. Shi and B. Xu, *Chem. Rev.*, 2015, **115**, 13165-13307.
11. E. R. Draper and D. J. Adams, *Chem*, 2017, **3**, 390-410.
12. Z. Sun, Q. Huang, T. He, Z. Li, Y. Zhang and L. Yi, *ChemPhysChem*, 2014, **15**, 2421-2430.
13. J. Mayr, C. Saldías and D. Díaz Díaz, *Chem. Soc. Rev.*, 2018, **47**, 1484-1515.
14. M. D. Segarra-Maset, V. J. Nebot, J. F. Miravet and B. Escuder, *Chem. Soc. Rev.*, 2013, **42**, 7086-7098.
15. F. Rodríguez-Llansola, B. Escuder and J. F. Miravet, *J. Am. Chem. Soc.*, 2009, **131**, 11478-11484.
16. M. O. Guler and S. I. Stupp, *J. Am. Chem. Soc.*, 2007, **129**, 12082-12083.
17. N. Singh, M. P. Conte, R. V. Ulijn, J. F. Miravet and B. Escuder, *Chem. Commun.*, 2015, **51**, 13213-13216.
18. M. Tena-Solsona, J. Nanda, S. Díaz-Oltra, A. Chotera, G. Ashkenasy and B. Escuder, *Chem. Eur. J.*, 2016, **22**, 6687-6694.
19. S. Bhowmick, L. Zhang, G. Ouyang and M. Liu, *ACS Omega*, 2018, **3**, 8329-8336.
20. F. Rodríguez-Llansola, J. F. Miravet and B. Escuder, *Chem. Commun.*, 2009, **0**, 7303-7305.
21. N. Singh and B. Escuder, *Chem. Eur. J.*, 2017, **23**, 9946-9951.
22. N. Singh, K. Zhang, C. A. Angulo-Pachon, E. Mendes, J. H. van Esch and B. Escuder, *Chem. Sci.*, 2016, **7**, 5568-5572.
23. M. Häring, A. Abramov and D. Díaz Díaz, *Macromol. Symp.*, 2017, **372**, 87-101.
24. F. Galindo, M. Isabel Burguete, R. Gavara and S. V. Luis, *J. Photochem. Photobiol. A*, 2006, **178**, 57-61.
25. R. Otter, C. M. Berac, S. Seiffert and P. Besenius, *Eur. Polym. J.*, 2019, **110**, 90-96.
26. Y. You, *Org. Biomol. Chem.*, 2018, **16**, 4044-4060.
27. D. E. J. G. J. Dolmans, D. Fukumura and R. K. Jain, *Nat. Rev. Cancer*, 2003, **3**, 380-387.
28. M. I. Burguete, F. Galindo, R. Gavara, S. V. Luis, M. Moreno, P. Thomas and D. A. Russell, *Photochem. Photobiol. Sci.*, 2009, **8**, 37-44.
29. C. Felip-León, C. Arnau Del Valle, V. Pérez-Laguna, M. Isabel Millán-Lou, J. F. Miravet, M. Mikhailov, M. N. Sokolov, A. Rezusta-López and F. Galindo, *J. Mater. Chem. B*, 2017, **5**, 6058-6064.
30. D. C. Neckers, *J. Photochem. Photobiol. A*, 1989, **47**, 1-29.
31. C. Li, F. Lin, W. Sun, F. G. Wu, H. Yang, R. Lv, Y. X. Zhu, H. R. Jia, C. Wang, G. Gao and Z. Chen, *ACS Appl. Mater. Interfaces*, 2018, **10**, 16715-16722.
32. S. Sharma and A. Sharma, *Org. Biomol. Chem.*, 2019, **17**, 4384-4405.
33. P. Li and G.-W. Wang, *Org. Biomol. Chem.*, 2019, **17**, 5578-5585.

34. M. I. Burguete, R. Gavara, F. Galindo and S. V. Luis, *Catal. Commun.*, 2010, **11**, 1081-1084.
35. R. Alcántara, L. Canoira, P. G. Joao, J. G. Rodriguez and I. Vázquez, *J. Photochem. Photobiol. A*, 2000, **133**, 27-32.
36. J. H. Day, *Chem. Rev.*, 1963, **63**, 65-80.
37. A. Seeboth, D. Lötzsch, R. Ruhmann and O. Muehling, *Chem. Rev.*, 2014, **114**, 3037-3068.
38. A. Seeboth, J. Kriwanek and R. Vetter, *J. Mater. Chem.*, 1999, **9**, 2277-2278.
39. S. Srinivasan, P. A. Babu, S. Mahesh and A. Ajayaghosh, *J. Am. Chem. Soc.*, 2009, **131**, 15122-15123.
40. A. Seeboth, J. Kriwanek and R. Vetter, *Adv. Mater.*, 2000, **12**, 1424-1426.
41. U. Maitra, S. Mukhopadhyay, A. Sarkar, P. Rao and S. S. Indi, *Angew. Chem. Int. Ed.*, 2001, **40**, 2281-2283.
42. T. Yi, K. Sada, K. Sugiyasu, T. Hatano and S. Shinkai, *Chem. Commun.*, 2003, **39**, 344-345.
43. H. Koizumi, Y. Kimata, Y. Shiraishi and T. Hirai, *Chem. Commun.*, 2007, **43**, 1846-1848.
44. A. Torres-Martínez, C. A. Angulo-Pachón, F. Galindo and J. F. Miravet, *Soft Matter*, 2019, **15**, 3565-3572.
45. M. Fontanillo, C. A. Angulo-Pachón, B. Escuder and J. F. Miravet, *J. Colloid Interface Sci.*, 2013, **412**, 65-71.
46. C. A. Angulo-Pachon and J. F. Miravet, *Chem. Commun.*, 2016, **52**, 5398-5401.
47. R. Sjöback, J. Nygren and M. Kubista, *Spectrochimica Acta Part A: Molecular Spectroscopy*, 1995, **51**, L7-L21.
48. U. Opriel, K. Seikel, R. Schmidt and H. D. Brauer, *J. Photochem. Photobiol. A*, 1989, **49**, 299-309.
49. M. E. Daraio and E. San Román, *Helv. Chim. Acta*, 2001, **84**, 2601-2614.

Supporting Information

Adsorption of Rose Bengal on a self-assembled fibrillar network affords a thermally switchable oxygenation photocatalyst and a thermochromic soft material

*Carla Arnau-del-Valle, Carles Felip-León, César A. Angulo-Pachón, Francisco Galindo and Juan F. Miravet**

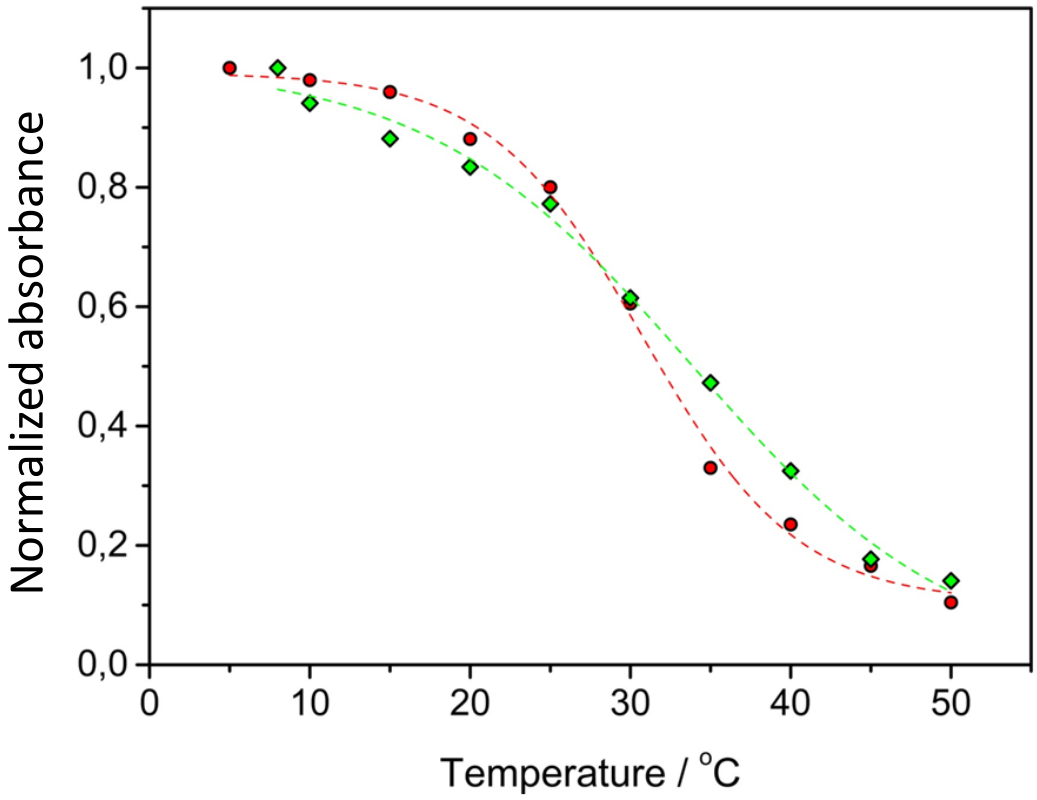

Figure S1. UV-vis absorption measurements of the light scattering produced by the gels in CH_2Cl_2. at 800 nm, used to obtain the melting temperatures (T_{gel}). Red circles: **1**, green diamonods: **1**+ RB. [RB] = 7.7 µM, [**1**] = 14.4 mM

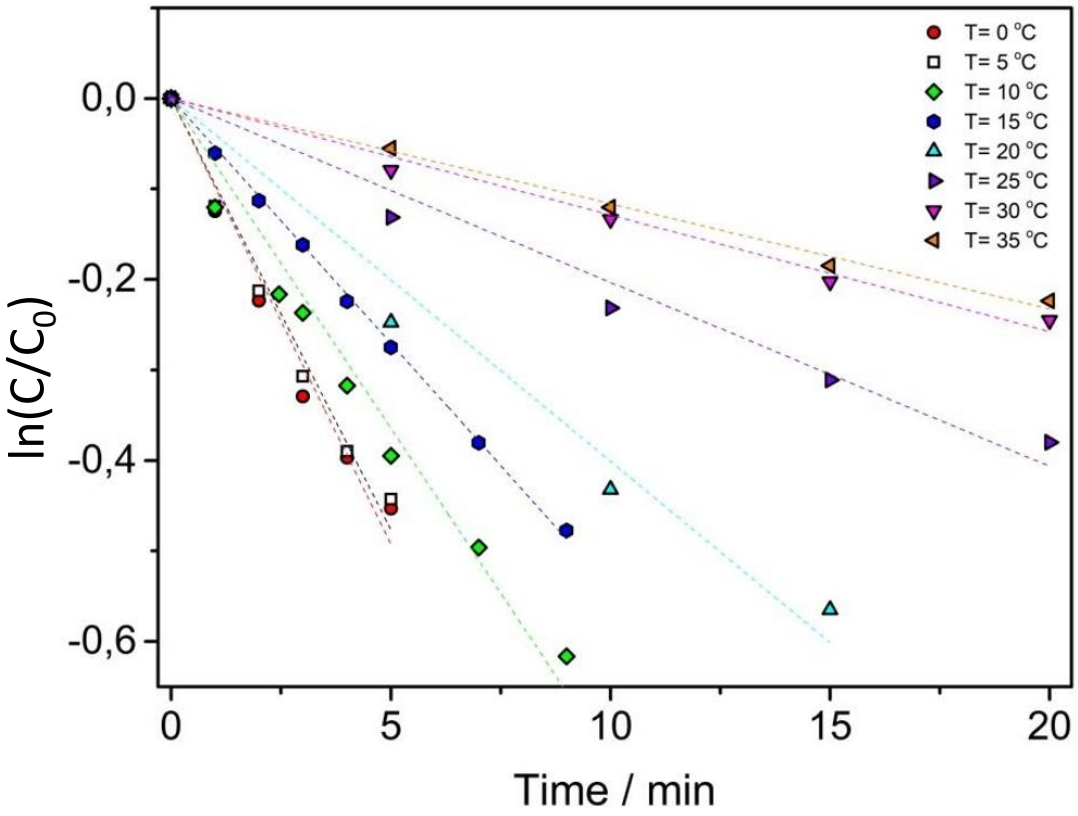

Figure S2. Kinetic data for singlet oxygen generation of RB+**1** at different temperatures. [RB] = 7.7 µM, [**1**] = 14.4 mM in CH_2Cl_2. ΔT = 5 ºC

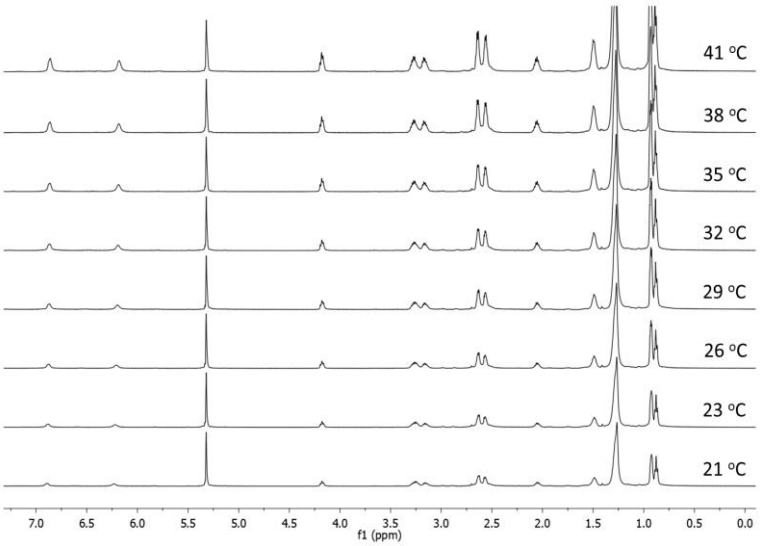

Figure S3. NMR spectrum of **1** at different temperatures.

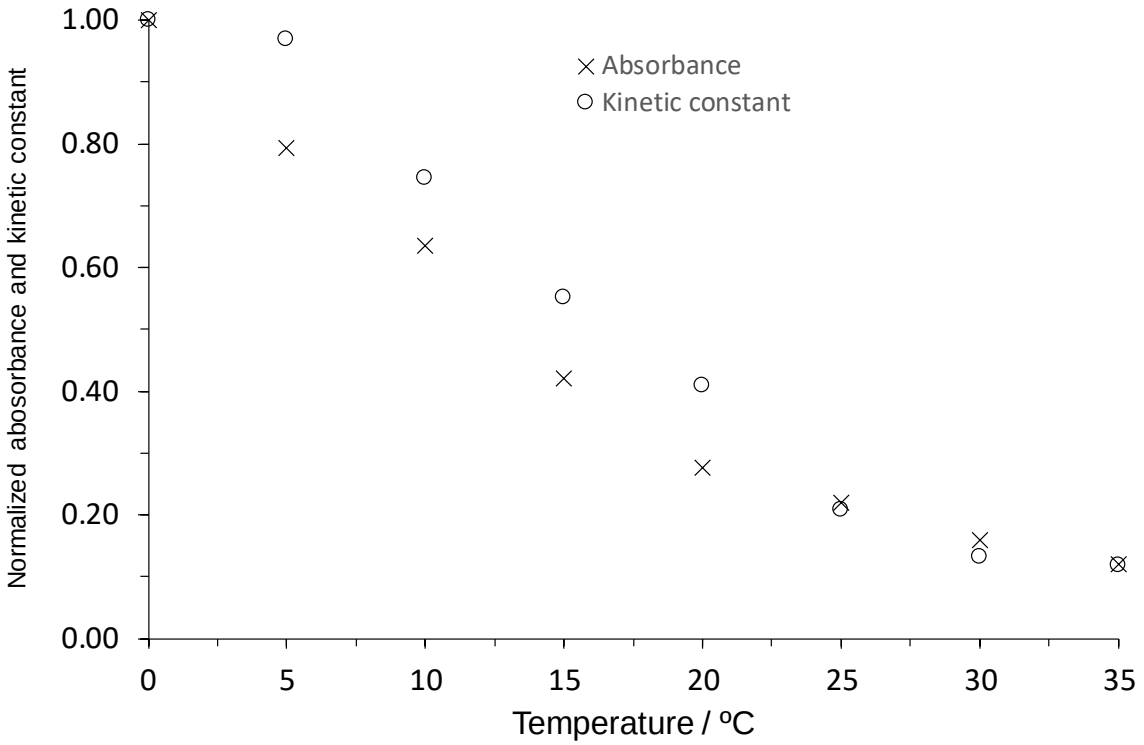

Figure S4. Comparison of absorbance at 560 nm $^1O_2$ production rate for the system **1**-RB at different temperatures. [RB] = 7.7 μM, [**1**] = 14.4 mM in CH_2Cl_2.